# CFD Predictions of Induced Fluid Forces and Dynamic Coefficients for a Compressor Eye Seal

Mohamed KAMOUNI
Sidi Mohamed ben Abdelleh University, Fez, Morocco

**Abstract**—Labyrinth seals are widely used in gas compressors to reduce internal leakage and increase the compressor efficiency. Due to the eccentricity between the rotating impeller and the stationary part as well as the shaft whirling motion, forces are generated when the leakage flow passing through these seals. These driving forces act on the rotor and may modify its dynamic stability. Thus, accurate predictions of these forces become a very important task for compressor rotordynamic designs. This paper presents tri-dimensional CFD investigations to simulate driving forces and dynamic coefficients of an eccentric labyrinth seal generally used as a compressor eye seal. The seal has five tapered teeth fixed on the stator and the work fluid is air. The model accuracy has beencompared to previous Bulk Flow and CFX resultson the same seal. These comparison results concern the pressure distribution along the sealas well as radial force components at zero preswirl. Moreover, results about pressure distribution in the circumferential direction and velocity vectors are presented. Aditionally, a parametric study has been conducted to show the effects of the whirl frequencyalong with three inlet swirl velocities(negative, zero and positive) and three high shaft speeds on the rotordynamic characteristics of the seal. Obtained results show that zero or moderate negative inlet swirl velocities are benifical from a point of view dynamic stability of the seal and therotordynamic coefficients have to be considered whirlingfrequency-dependent at high rotor speed rates.

**Index Terms**— Labyrinth seal, Dynamic stability, Rotor dynamic coefficients, CFD, Inlet swirl, Whirl frequency

## 1 INTRODUCTION

INresponse to the constantly increasing demand for higher levels of productivity, modern turbomachines are designed to be more efficient. They should run at higher speeds, higher pressures, tighter clearances, and last longer. As a particular component improving performance of such machines, annular gas seals are key elements to reduce leakage flows between rotating and stationary parts of turbomachines. These elements are effective not only on the system damping but even on the system stiffness, strongly affecting both the rotor stability and the position of the rotor first natural frequency [1, 2]. It has been proven that annular seals dynamic instability can lead to serious damage if not properly controlled.

Labyrinth seals, the most common type of annular gas seals, are widely used in turbomachinery including gas turbines, turbo pumps and compressors. Figure 1 illustrates typical labyrinth seals integrated in a multi-stage centrifugal compressor. These seals are composed of a series of circular blades and annular grooves which present a tortuous path for flow of the process fluid. The working principle of a labyrinth seal consists in separating regions at different pressures through the clearance where the conversion of pressure energy into kinetic energy occurs. The latter can then be dissipated into thermal energy in the cavity downstream the clearance or transferred to the next gap through the kinetic carryover [3]. The major advantages of labyrinth seals are their simplicity, reliability, and tolerance to large thermal and pressure variations [4]. Although labyrinth seals have been confirmed to be a major source of driving forces resulting in rotor instability problems, they remain the common sealing solution in compressors and turbines as balance drum, interstage, center, shaft end, and impeller eye seals. Due to the many geometrical and physical influence factors on the rotordynamic characteristics of labyrinth gas seals and their decisive influence on the dynamic stability of turbomachines, worldwide researchers have conducted a large number of experimental and theoretical investigations focused on measuring and predicting the rotordynamic coefficients for this kind of seals. However, various disagreements have been reported between predictions and real measurements on the rotor dynamic behaviour of these seals [5 - 7]. Thus, accurate prediction of fluid induced forces and rotor dynamic coefficients remains a demanding and challenging task for labyrinth gas seals [8].

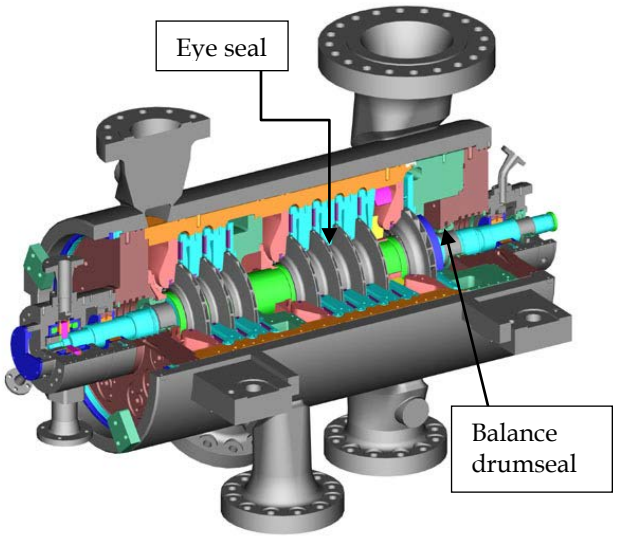


Fig.1. Typical labyrinth seals in a multi-stage centrifugal compressor

Currently, there are two known solutions to predict dynamic characteristics of labyrinth gas seals, the bulk flow and CFD methods.

The bulk flow models were developed in the early 1980s to predict dynamic characteristics of annular seals and these models continue to be used in the industry [9]. Iwatsubo [10] is among the first authors which developed bulk-flow approach. Subsequently, to assess its predictions accuracy, Childs and Scharrer [11, 12] compared bulk flow calculations within labyrinth seals to experimental measurements. Due to the complex geometry of labyrinth seals, the bulk-flow method needs to simplify the physical problem models and governing equations as wellto obtain approximate and quick results. Therefore, this approach yields good results for plain annular seals but poor predictions when recirculation is present in the flow field [13]. To improve the bulk flow model, multiple control volume techniques have been used that divide the geometry of the seal [14]. These techniques associated dominant flow behavior into different control volumes which are then linked by appropriate boundary conditions. However, a priori knowledge of the flow required parameters is not always known and the interface conditions change for different seal operating conditions. In this context, to improve bulk flow predictions in labyrinth seals, Kirk [15] has developed a method to calculate inlet swirl velocity which it has been proven that it affects strongly the dynamic stability of the rotor. Furthermore, these models require some empirical relationships such as Hirs and Moody friction factor relationships to quantify shear stress in a developed turbulent pipe flow [16, 17]. These empirical coefficients have been the subject of many investigations [18, 19] to formulate an accurate model for them. However, it is difficult to capture the full nature of the friction factor through bulk flow models without an experimental measurement for each seal [20].

Unlike bulk flow model, computational fluid dynamic "CFD" does not rely on empirical wall and interface constants that may change for varying applications and geometry. In addition to this, the exact geometry of the seal may be modelled allowing optimization of the teeth profile. However, the obvious drawback of CFD compared to bulk-flow is increased computational requirement. The present research attempts to calculate the induced forces acting on the rotor and the dynamic characteristics of an eccentric labyrinth gas seal based on tridimensional CFD techniques solving the general Reynolds Averaged Navier-Stokes equations along with appropriate turbulence model.

## 2 Seal Geometry and Computational Model

### 2.1 Seal Geometry

The labyrinth gas seal object of this work has five tapered teeth fixed on the stator lateral surface. This kind of seals is generally used as impeller eye seal in multi-stage centrifugal compressors to limit secondary flows. The seal's mean radial clearance is **C**=0.292 mm and its relative eccentricity is **ε = e/C** = 0.1 where **e** is the orbital motion radius. The 2-D seal geometry is shown in figure 1.

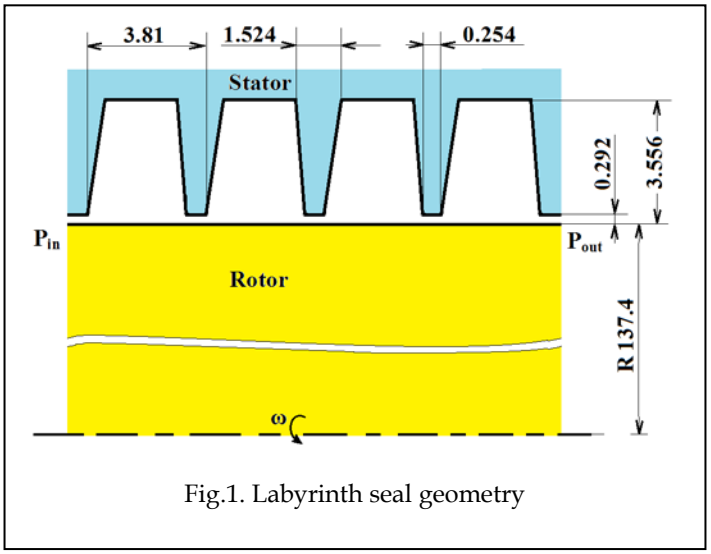


Fig.1. Labyrinth seal geometry

The seal working fluid is air. A cut section of the 3-D fluid computational domain is shown in figure 2.The teeth are represented by circumferential grooves in this computational domain.

Fig.2. A cut section of the 3-D computational domain of the seal

### 2.2 Governing Equations

The turbulent flow through the seal is governed by the continuity and momentum equations.

**Continuity equation:**

$$\frac{\partial \rho}{\partial t} + \frac{\partial (\rho u_i)}{\partial x_i} = 0 \qquad (1)$$

**Momentum equation:**

$$\frac{\partial \rho u_i}{\partial t} + \frac{\partial (\rho u_i u_j)}{\partial x_j} = -\frac{\partial P}{\partial x_i} + \frac{\partial}{\partial x_j}\left[\mu_{eff}\left(\frac{\partial u_i}{\partial x_j} + \frac{\partial u_j}{\partial x_i}\right)\right] + S_M (2)$$

where

$S_M$ is the sum of body forces

$\mu_{eff}$is the effective viscosity accounting for turbulence.

$$\mu_{eff} = \mu + \mu_t \qquad (3)$$

$\mu_t$ is the turbulence viscosity and μ is a constant.

These equations are completed by the (k, ω) SST turbulence

model.

### 2.3 Meshing Procedure

Hexahedral mesh elements were used to create three dimensional non-uniform structured meshes in the entire computational domain. An adequate mesh refinement is allowed to the clearance area and boundary layers to accurately calculate desired physical parameters of the flow within the seal. Fig. 5 shows a cut section of generated computational grids in the 3-D computational domain.

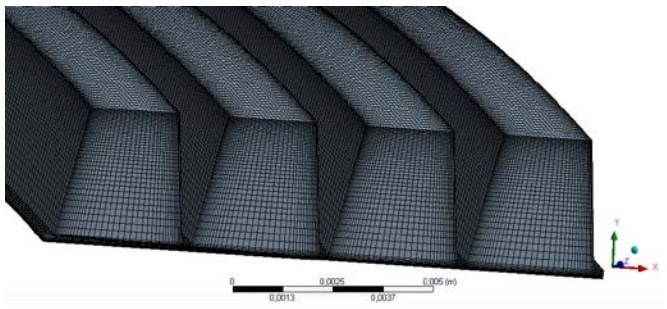

Fig.4. A cut section of the 3-D Mesh used for the fluid computational domain of the seal

### 2.4 Frame Transfer from Stationary to Rotating

Observing the motion of rotor-seal system from a stationary frame, the rotor is spinning at the speed ω while also whirling at the speed Ω at the same time, which means that the location of rotor and thus the shape of mesh are changing all the time. So, it is actually a transient problem involved with mesh moving. To avoid a transient analysis and moving mesh, a rotating frame with the speed Ω was applied as shown in figure 5. In the rotating frame, the rotor itself spins at the speed (ω-Ω), while the stator spins at the speed Ω in the opposite direction to the frame. Thus it becomes a steady state problem and there is no mesh moving.

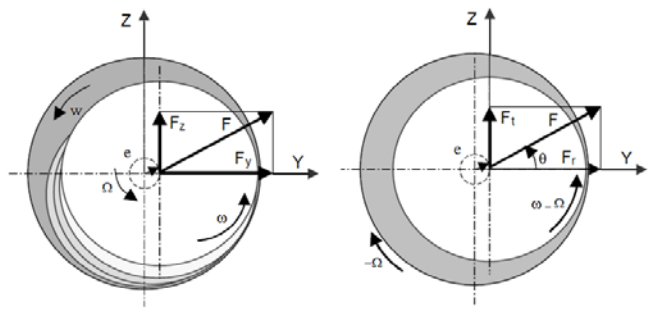


Fig.5. Frame transfer from stationary to rotating

### 2.5 Induced Forces and Rotordynamic Coefficients

The fluid driving forces exerted on the rotor can be obtained at each whirl frequency Ω by integration of the static pressure along and around the seal rotor surface.

$$F_y = R\iint p\cos\theta\, d\theta\, dx \tag{4}$$

$$F_z = R\iint p\sin\theta\, d\theta\, dx \tag{5}$$

For small motion of the rotor center about a centered position, the relation between the reaction-force components and the shaft motion is defined by the following linearized dynamic model where the added mass terms are neglected.

$$-\begin{Bmatrix} F_y \\ F_z \end{Bmatrix} = \begin{bmatrix} K & k \\ -k & K \end{bmatrix}\begin{Bmatrix} y \\ z \end{Bmatrix} + \begin{bmatrix} D & d \\ -d & D \end{bmatrix}\begin{Bmatrix} \dot{y} \\ \dot{z} \end{Bmatrix} \tag{6}$$

where (y, z) define the lateral motion of the rotor center relative to the stator, (Fy , Fz) are the components of the reaction force acting on the rotor. (K, k) and (D, d) represent the direct and cross-coupled stiffness and damping coefficients, respectively. The cross-coupled terms (k, d) arise from the fluid's circumferential velocity component. The rotor whirling motion is referred to as self-excited rotordynamic instability. It has been proven that cross-coupling stiffness effects tend to sustain whirling motion in annular seals at a subsynchronous natural frequency when insufficient damping is present [21].

If the shaft center moves in a circular orbit with radius e, then the rotation displacement vector to the shaft center has coordinates:

$$y = e\cos(\Omega t) \tag{7}$$

$$z = e\sin(\Omega t) \tag{8}$$

The radial force component $F_r$ and the tangential force component $F_t$can be formulated as follows:

$$\frac{F_r(\Omega)}{e} = \frac{F_y(t=0)}{e} = -d\,\Omega - K \tag{9}$$

$$\frac{F_t(\Omega)}{e} = \frac{F_z(t=0)}{e} = k - D\Omega \tag{10}$$

The direct stiffness coefficient **K** and the cross-coupled damping coefficient **d** can be obtained employing a linear regression of the calculated radial force for two different values of Ω in equation (9). The direct damping coefficient **D** and the cross-coupled stiffness coefficient **k** can be determined from linear regression of the calculated tangential force for two different values of Ω in equation (10).

## 3 Results and Discussions

### 3.1 Assessment of the CFD Predictions Accuracy

The developed model has been solved in the given seal

respecting the boundary and operating conditions used by [22 and 23] and summarized in table1.The static pressure distribution along the seal has been locally computed in the seal mid-cavities and theradial and tagential force components have been also calculated for five whirling ratios (Ω/ω=0, 0.25, 0.5, 0.75, and 1).

Figure6shows a comparison between the current CFD predictionsof the axial pressure distribution andprevious resultsof Kirk and Gao [23]on the same seal using separately bulk Flow and CFX models. This figure shows a good agreement between CFD predictionsand calculation results ofKirk and Gao. Additionally, this figure shows that the pressure drops from the inlet pressure at left to the outlet pressure at right. The pressure drop mainly occursat the tips of teethand the pressure is almost equal in the same cavity interior.

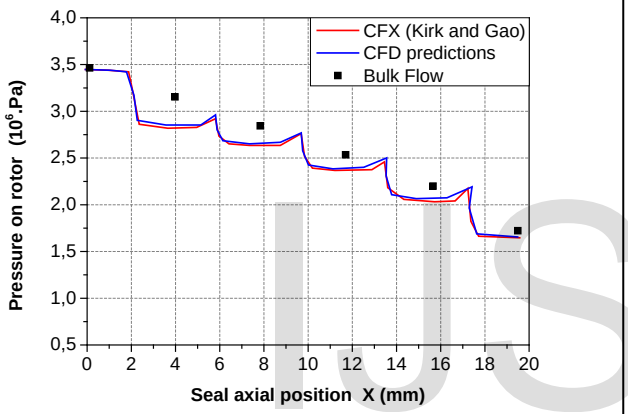


Fig.6. CFD compared to previous predictions of the pressure distribution in the axial direction of the seal

Figures 7 and 8 represent respectively the radial and the tangential force componentes versus the whirling ratio.The interceptsare direct stiffness and cross-coupled stiffness in figures 7 and 8, respectively. The slopes are cross-coupled dampingand direct damping in figures 7 and 8, respectively. Figure 7 shows that the threemethods provide nearely the same slope and lead to the same cross-coupled damping but differentdirect stiffness coefficients. This difference can be neglected because direct stiffnessand cross-coupled damping are less important from a rotor stability point on view.However, figure8 shows good agreement for cross-coupledstiffness and direct damping among the three models.

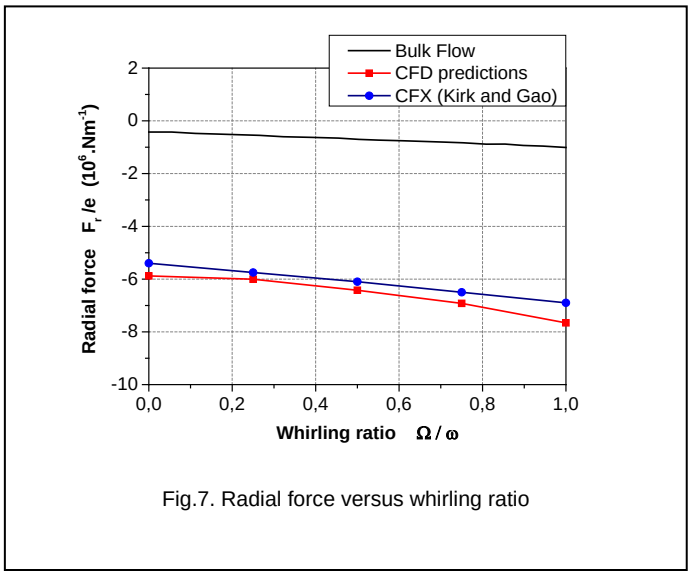


Fig.7. Radial force versus whirling ratio

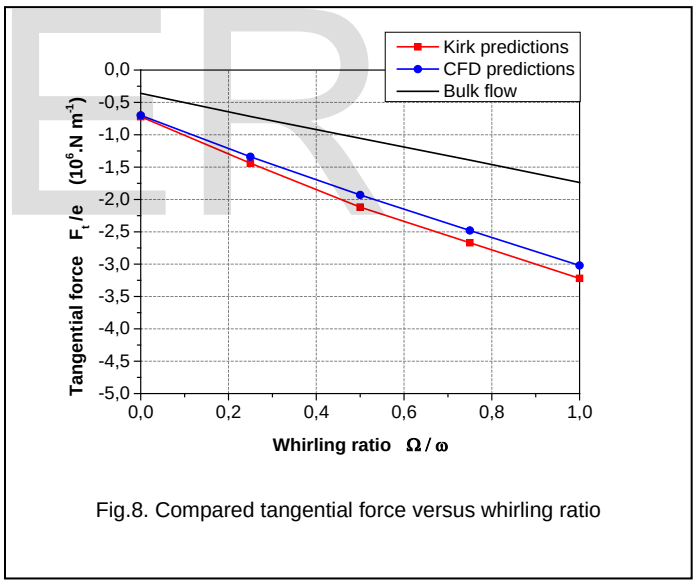


Fig.8. Compared tangential force versus whirling ratio

### 3.2 Flow Structure Details in the Seal

Figure 9 shows contours of the static pressure in an axial radial plane of the seal. One can easily see that pressure drop starts at the seal inlet and continues at each tooth throttling to rich the outlet pressure at the seal exit. Furthermore, the quasi same color in each cavity interior confirms that the pressure is quasi constant in each cavity interior.

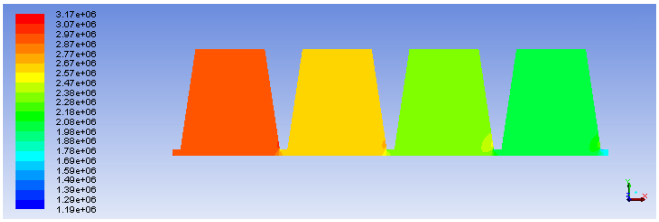

Fig.9. Pressure contours in the XY plane of the seal

Figure 10 shows the velocity vectors in an axial radial plane of the seal. The high pressure drop occurs in the first cavity where a strong flow jet is generated making the flow more turbulent in this cavity. We note the presence of recirculation zones in the seal cavities. These vortexes act as brakes to stop the axial velocity of the flow through the seal and therefore to reduce the leakage flow.

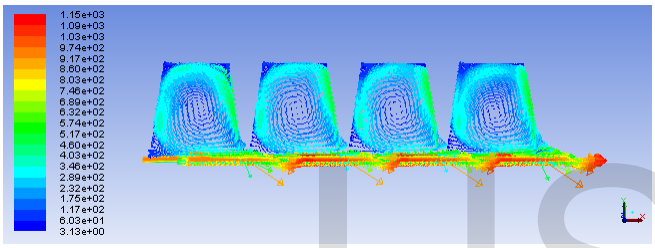

Fig.10. Velocity vectors in the XY plane of the seal

Figure 11 shows the static pressure distribution in the circumferential direction of the seal. It is shown that the pressure fluctuations are almost sinusoidal in every cavity.

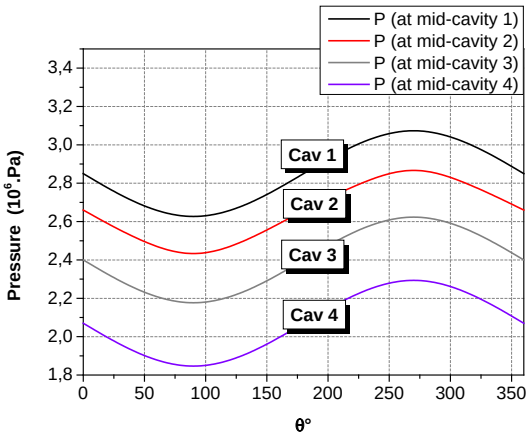


Fig.11. Pressure distribution in the circumferential direction at each mid-cavity of the seal

### 3.3 Effects of Inlet Swirl Ratio and Whirling Ratio on Dynamic Coefficients

Figure 12represents the direct stiffness coefficient versus whirling ratio with the inlet swirl ratio as a parameter. This figure shows that direct stiffness decreases with increasing whirling ratio but it decreases slightly withpreswirl ratio increasing.

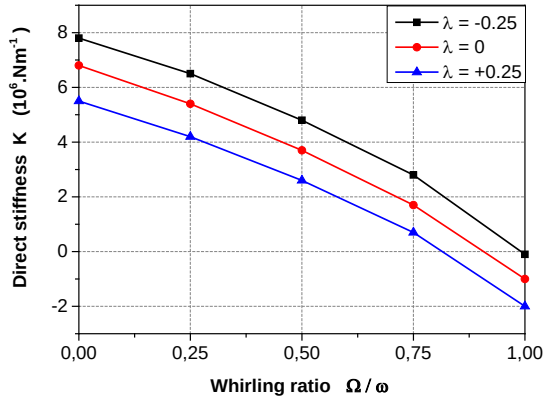


Fig.12. Direct stiffness coefficient versus whirling ratio with the inlet swirl ratio as a parameter

Figure 13 shows that cross-coupled stiffness coefficient is practically not influenced by whirling ratio variations. Namely, cross stiffness coefficient is whirling frequency-independent. However, it is of interest to note that the cross-coupled stiffness changes from the positive sign to the negative one when the preswirl ratio changes also from positive value (0.25) to negative one (−0.25). Since negative cross stiffness becones a stabilizing influence, it can be stated that negative inlet swirl is benifical in dynamic stability point of view for this seal.

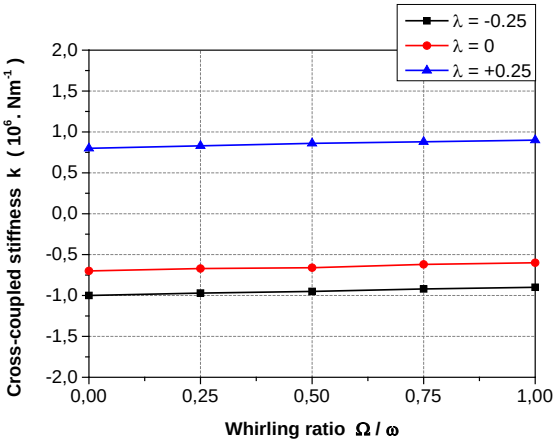


Fig.13. Cross coupled stiffness coefficient versus whirling ratio with the inlet swirl ratio as a parameter

Figure 14 shows that direct damping coefficient increaseswith increasing preswirl ratio but it increases weakly with increasing whirling ratio.Direct damping is a stabilizing influence, so maximum values are desirable for this coefficient. Namely, high preswil ratios provide high direct damping to keep the seal dynamically more stable.

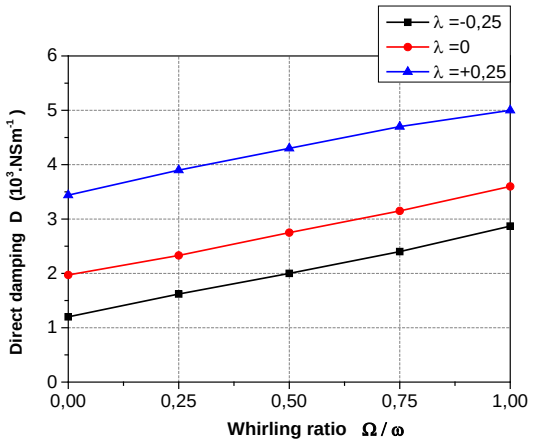


Fig.14. Direct damping coefficient versus whirling ratio with the inlet swirl ratio as a parameter

Figure 15 shows that cross-coupled damping coefficient increases slightly with increasingpreswirlratio but decreases weakly with increasing whirling ratio. Furthermore, it is proven that this coefficient has only little influence on the rotor stability. Thus, small fluctuations in this coefficient are without big interest.

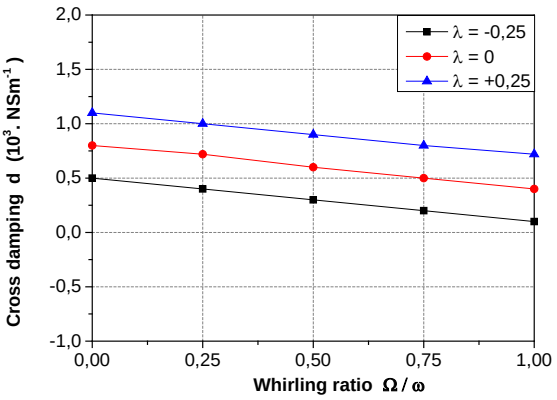


Fig.15. Cross coupled damping coefficient versus whirling ratio with the inlet swirl ratio as a parameter

To compare the destabilizing influence of cross-coupled stiffness to the stabilizing influence of direct damping, the whirl frequency ratio σ is introduced as follows:

$$\sigma = \frac{k}{D\Omega} \qquad (11)$$

This ratio provides an assessment for the dynamic stability of the seal. More the whirl frequency ratio is smaller more the seal is dynamically stable.Figure 16 shows that the whirl frequency ratio is quite small for no preswirlandminimal for the negative preswirl case. Therfore, integration of swirl brakes at the seal inlet is more important to improve the dynamic stability of this kind of seals.

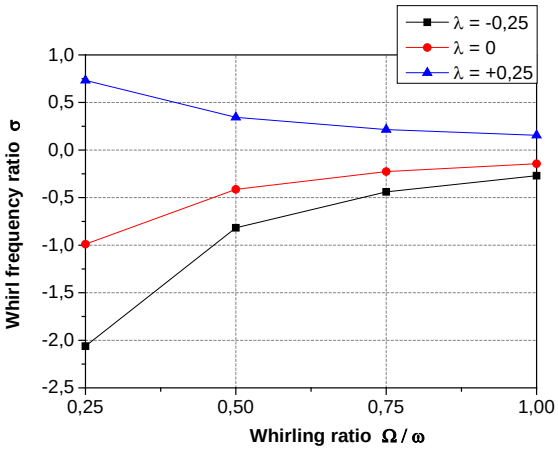


Fig.16. Whirl frequency ratio versus whirling ratio with the inlet swirl ratio as a parameter

### 3.4 Effects of Rotor Speed and Whirling Ratio on Dynamic Coefficients

As shown in the last section (**3.3**), at the given rotor speed (**ω** = 11097 rpm) and for different preswil velocities, the direct stiffness coefficient is sensitive to the whirling ratio variations. However, this ratio has a slight influence on the direct and cross-coupled damping coefficientsand only a very weak influence on the cross-coupled stiffness. Namely, except for direct stiffness, direct and cross damping and cross stiffness can be considered whirling frequency-independent in the given predictions range. So, it's of interest to show the effect of whirling ratio on dynamic coefficients at high rotor speed cases.

Figures 17, 18, 19, and 20 represent at zero preswirlrespectively direct stiffnes, cross-coupled stiffness, direct damping, and cross-coupled damping coefficients versus the whirling ratio with the rotor speed as a parameter. It can be easily seen thatat high rotor speeds (ω ≥ 15500 rpm), these dynamic coefficients become more influenced by the whirl frequency and they have to be considered whirling frequency-dependent.

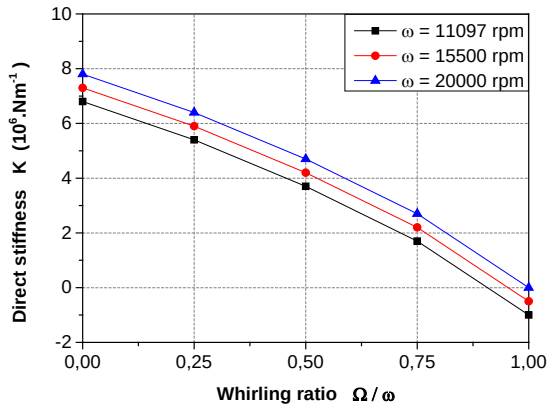


Fig.17. Direct stiffness coefficient versus whirling ratio at zero preswirlwith the rotor speed as a parameter

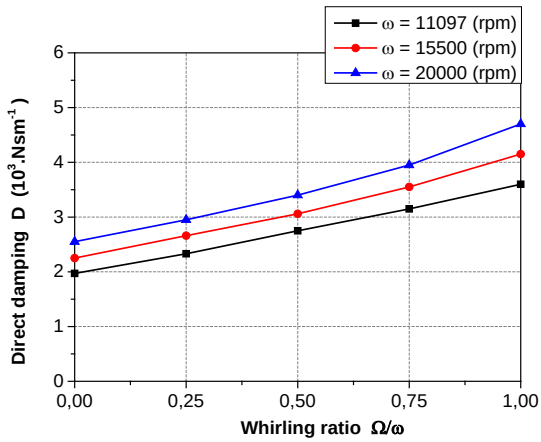


Fig.19. Direct damping coefficient versus whirling ratio at zero preswirlwith the rotor speed as a parameter

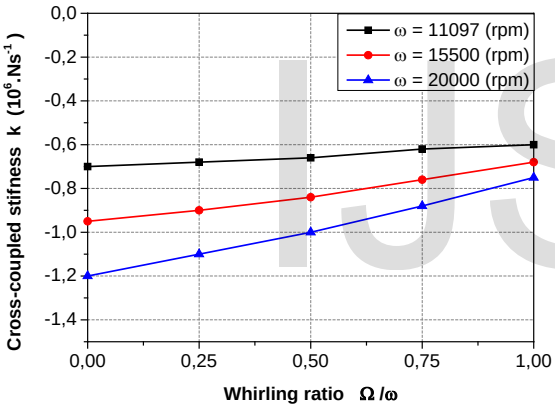


Fig.18. Cross stiffness coefficient versus whirling ratio at zero preswirlwith the rotor speed as a parameter

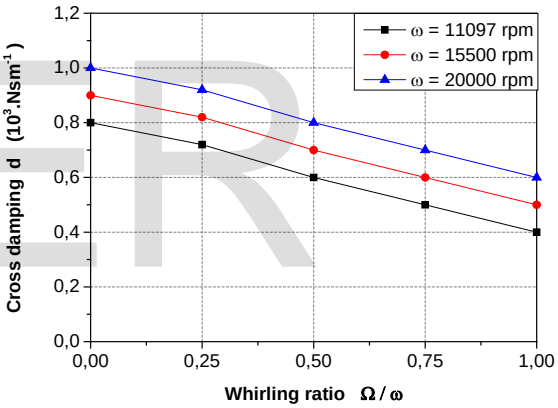


Fig.20. Cross damping coefficient versus whirling ratio at zero preswirlwith the rotor speed as a parameter

## 4 Conclusion

A CFD model has been developed to predict induced fluid forces and dynamic coefficients in labyrinth gas seals. Themodel solves the general Reynolds Averaged Navier-Stokes equations along with the k-ω SST turbulence modelrespectinggiven boundary and operating conditions.The model predictions accuracy has been compared to previous results of Kirk and Gao on the same seal using separately Bulk Flow and CFX methods to calculate pressure distribution and driving force components at zero preswirl.Then, the effects of inlet swirl (negative, zero, and positive), whirl frequency, and high rotor speedshave been investigated on thedynamic characteristicsof theseal. Through the in-depth research and analysis, someconclusions are summarized as follows:

- Pressure drops from the inlet to the outlet pressures. The

pressure drop mainly occursat the tips of teethand the pressure is almost equal in the same cavity interior

- The high pressure drop occurs in the first cavity where a strong flow jet is generated making the flow more turbulent in this cavity. We note the presence of recirculation zones in the seal cavities. These vortexes act as brakes to stop the axial velocity of the flow through the seal.
- With no preswirl or moderate negative preswirl,the seal isdynamically more stable. Therefore, integration of swirl brakes at the seal inlet is more important to improve the dynamic stability of this kind of seals.
- At the rotor speed ($\omega$ = 11097 rpm), direct and cross-coupled damping and cross-coupled stiffness coefficientsare very slightly influenced by the whirling ratio variations and can be considered whirling frequency-independent.
- At high rotor speeds ($\omega \geq$ 15500 rpm), stiffness and damping dynamic coefficients become more influenced by the whirl frequency and they have to be considered whirling frequency-dependent.

## References

[1] D. W., Childs, and J. M., Vance, "Annular Seals as Tools to Control Rotordynamic Response of Future Gas Turbine Engines," 30th Joint Propulsion Conference and Exhibit, AIAA Paper 1994-2804, 1994.

[2] D.W., Childs, and J. M., Vance, "Annular Seals and the Rotordynamics of Compressors and Turbines," Proceedings of the 26th Turbomachinery Symposium, Turbomachinery Lab., Texas A&M Univ., College Station, TX, Sept. pp. 201–220, 1997.

[3] T., Weinberger, K., Dullenkopf, and H. J., Bauer, "Influence of Honeycomb Facings on the Temperature Distribution of Labyrinth Seals," ASME Paper No. GT2010-22069, 2010.

[4] R. E., Chupp, R. C., Hendricks, S. B., Lattime, and B. M., Steinetz, "Sealing in Turbomachinery," J. Propul. Power, 22(2), pp. 313–349, 2006.

[5] J., Pelletti, "A Comparison of Experimental Results and Theoretical Predictions for the Rotordynamic Coefficients of Short (L/D _ 1/6) Labyrinth Seals," M.S. Thesis, Texas A&MUniv., College Station, TX, 1990.

[6] A., Picardo, and D.W., Childs, "Rotordynamic Coefficients for a Tooth-on-Stator Labyrinth Seal at 70 Bar Supply Pressures: Measurements Versus Theory and Comparisons to a Hole-Pattern Stator Seal," Journal of Engineering for Gas Turbines and Power, Vol. 127, No. 4, pp. 843–855, 2005.

[7] D. W., Childs, J. E., Mclean, M., Zhang, and S. P., Arthur, "Rotordynamic Performance of a Negative-Swirl Brake for a Tooth-on-Stator Labyrinth Seal," American Soc. of Mechanical Engineers Paper GT2014-25577, 2014.

[8] M., Wensheng, C., Zhaobo, and J., Yinghou, "Leakage and Whirl Speed Study in Labyrinth Seal Using CFD", International Conference on Electronic & Mechanical Engineering and Information Technology (EMEIT), Harbin, China,Aug. 12–14, pp. 592-595, 2011.

[9] M. Arghir and J. Frêne, "A Bulk-Flow Analysis of Static and Dynamic Characteristics of Eccentric Circumferentially-Grooved Liquid Annular Seals," ASME J. Tribol., 126(2), pp. 316–325, 2004.

[10] T. Iwatsubo, "Evaluation of Instability Forces of Labyrinth Seals in Turbines or Compressors," In Proc. Rotordynamic Instability Problems in High Performance Turbomachinery, " NASA CP-2133, Texas A&M University, pp 139-167, 1980.

[11] D. W.Childs and J. K. Scharrer, ''AnIwatsubo Based Solution for Labyrinth Seals: A Comparison to Experimental Results,'' ASME J. Eng. Gas Turbines Power, 108, pp. 325–331, 1986.

[12] D.W. Childs and J.K. Scharrer, "TheoryVersus Experiment for the Rotordynamic Coefficients of Labyrinth Gas Seals: Part II— A comparison to Experiment," Journal of Vibration, Acoustics, Stress, and Reliability in Design, 110(3), pp 281-287, 1988.

[13] J. J. Moore and A. B. Palazzolo ''CFD Comparison to Three- Dimensional Laser Anemometer and Rotordynamic Force Measurements for Grooved Liquid Annular Seals,'' presented at the ASME/STLE International Tribology Conference, Oct. 1998, pp. 25–29, Toronto, Ontario, Canada, 1998.

[14] J. K. Scharrer, "Theory versus experiment for the rotordynamic coefficient of labyrinth gas seals: Part a two control volume model, " Journal of Vibration, Acoustics, Stress, and Reliability in Design, Trans. ASME, 110, pp. 270-280, 1988.

[15] R. G. Kirk, "A Method for Calculating Labyrinth Seal Inlet Swirl Velocity," Journal of Vibration and Acoustics, Trans.ASME, 112(3), pp 380- 383, 1990.

[16] G. G. Hirs, "A Bulk Flow Theory for Turbulent in Lubricant Films", Journal of Lubrication Technology, pp.137-146, 1973.

[17] L. Moody, "Friction Factors for Pipe Flow, " Transactions of the ASME, Vol. 66, pp. 671, 1944.

[18] A. M. Al-Qutub, D. Elrod, and H. W. Coleman, "A New Friction Factor Model and Entrance Loss Coefficient for Honeycomb Annular Gas Seals," ASME J. Tribology, 122(3), pp. 622–627, 2000.

[19] M. Arghir, F. Billy, G. Pineau, J. Frêne, and A. Texier, "Theoretical Analysis of Textured Damper Annular Seals," ASME J. Tribology, 129(3), pp. 669–678, 2007.

[20] R. J. D'Souza and D.W. Childs, "A Comparison of Rotordynamic-Coefficient Predictions for Annular Honeycomb Gas Seals Using Three Different Friction-Factor Models," ASME J. Tribology, 124(3), pp.524–529, 2002.

[21] J. J., Moore, D.L., Ransom, and F., Viana, "Rotordynamic Force Prediction of Centrifugal Compressor Impellers Using Computational Fluid Dynamics", GT2007- 28121, ASME Turbo Expo 2007, Montreal, Canada, 2007.

[22] T., Hirano, Z., Guo, and R. G., Kirk "Application of Computational Fluid Dynamics Analysis for Rotating Machinery—Part II: Labyrinth Seal Analysis," *Journalof Engineering for Gas Turbines and Power*, **127**(4), pp 820–826, 2005.

[23] G., Kirk, and R., Gao, "Influence of Preswirl on Rotordynamic Characteristics of Labyrinth Seals," Tribol. Trans., 55(3), pp. 357–364, 2012.

.